

Damage at hydrogenated amorphous/crystalline silicon interfaces by indium tin oxide overlayer sputtering

B n dicte Demaurex, Stefaan De Wolf, Antoine Descoedres, Zachary Charles Holman, and Christophe Ballif

Citation: *Appl. Phys. Lett.* **101**, 171604 (2012); doi: 10.1063/1.4764529

View online: <http://dx.doi.org/10.1063/1.4764529>

View Table of Contents: <http://apl.aip.org/resource/1/APPLAB/v101/i17>

Published by the [American Institute of Physics](http://www.aip.org).

Related Articles

Laser-silicon interaction for selective emitter formation in photovoltaics. II. Model applications

J. Appl. Phys. **112**, 114907 (2012)

Laser-silicon interaction for selective emitter formation in photovoltaics. I. Numerical model and validation

J. Appl. Phys. **112**, 114906 (2012)

Influence of the pattern shape on the efficiency of front-side periodically patterned ultrathin crystalline silicon solar cells

J. Appl. Phys. **112**, 113107 (2012)

Aluminum oxide–n-Si field effect inversion layer solar cells with organic top contact

Appl. Phys. Lett. **101**, 233901 (2012)

Limiting efficiency of generalized realistic c-Si solar cells coupled to ideal up-converters

J. Appl. Phys. **112**, 103108 (2012)

Additional information on *Appl. Phys. Lett.*

Journal Homepage: <http://apl.aip.org/>

Journal Information: http://apl.aip.org/about/about_the_journal

Top downloads: http://apl.aip.org/features/most_downloaded

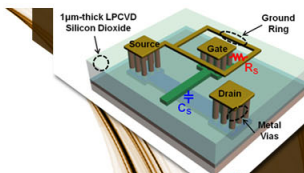
Information for Authors: <http://apl.aip.org/authors>

ADVERTISEMENT



**EXPLORE WHAT'S
NEW IN APL**

SUBMIT YOUR PAPER NOW!



SURFACES AND INTERFACES

Focusing on physical, chemical, biological, structural, optical, magnetic and electrical properties of surfaces and interfaces, and more...



ENERGY CONVERSION AND STORAGE

Focusing on all aspects of static and dynamic energy conversion, energy storage, photovoltaics, solar fuels, batteries, capacitors, thermoelectrics, and more...

Damage at hydrogenated amorphous/crystalline silicon interfaces by indium tin oxide overlayer sputtering

Bénédicte Demaurex,^{a)} Stefaan De Wolf, Antoine Descoeurdes, Zachary Charles Holman, and Christophe Ballif

École Polytechnique Fédérale de Lausanne (EPFL), Institute of Microengineering (IMT), Photovoltaics and Thin Film Electronics Laboratory, Rue A.-L. Breguet 2, CH-2000 Neuchâtel, Switzerland

(Received 12 July 2012; accepted 15 October 2012; published online 25 October 2012)

Damage of the hydrogenated amorphous/crystalline silicon interface passivation during transparent conductive oxide sputtering is reported. This occurs in the fabrication process of silicon heterojunction solar cells. We observe that this damage is at least partially caused by luminescence of the sputter plasma. Following low-temperature annealing, the electronic interface properties are recovered. However, the silicon-hydrogen configuration of the amorphous silicon film is permanently changed, as observed from infra-red absorbance spectra. In silicon heterojunction solar cells, although the as-deposited film's microstructure cannot be restored after sputtering, no significant losses are observed in their open-circuit voltage. © 2012 American Institute of Physics. [<http://dx.doi.org/10.1063/1.4764529>]

Silicon heterojunction (SHJ) solar cells have a high energy-conversion efficiency potential at reasonable cost.^{1,2} The emitter and back surface field are fabricated by depositing a few nanometers thin doped hydrogenated amorphous silicon (*a*-Si:H) layers on crystalline silicon (*c*-Si) wafer surfaces. Equally thin intrinsic *a*-Si:H buffer layers inserted between the wafer and these doped films significantly reduce the interface-state density.³ This enables the record-high open-circuit voltages (V_{oc} s) typically associated with these devices, and also high voltages at the maximum power point, needed for high fill factor values.^{4,5} As the lateral conductivity of the doped *a*-Si:H layers is rather poor, transparent conductive oxide (TCO) layers are deposited on the *a*-Si:H films. Ideally, these TCO layers simultaneously guarantee lateral charge transport to the external metal contacts, low contact resistance to the underlying doped *a*-Si:H layers, and maximal optical transmission into the active absorber, i.e., the *c*-Si wafer. Indium tin oxide (ITO) is often the TCO material of choice in SHJ devices and is usually deposited by reactive magnetron sputtering. For this technique, the flux and energy of particles significantly influence the growth and properties of the deposited films.⁶

Damage of *a*-Si:H layers by sputter-induced ion bombardment is known for decades,⁷ and may be of concern for high-efficiency SHJ device fabrication too. Regarding this, Table I shows the evolution of the effective carrier lifetime (τ_{eff}) and the so-called *implied*- V_{oc} during SHJ cell fabrication. The *implied*- V_{oc} is calculated from the excess carrier density generated under one-sun illumination in open-circuit conditions, and is indicative of the V_{oc} measured on finished devices. Directly after deposition of device-relevant intrinsic/doped *a*-Si:H stacks, a high carrier lifetime value is obtained without any post-deposition annealing. Following ITO sputtering, a severe drop of 76% in τ_{eff} and of nearly 30 mV in *implied*- V_{oc} can be observed, indicating indeed a loss in wafer passivation. Subsequent curing ($\sim 190^\circ\text{C}$ for a

few minutes) after screen printing the metal grid front electrode brings the finished-device V_{oc} almost fully back up to the initial *implied*- V_{oc} . These results confirm that TCO sputtering damages the *a*-Si:H/*c*-Si interface in SHJ structures,^{8,9} but that most of the damage is recovered by low-temperature annealing. In this paper, we first discuss the origin of the sputter damage. Second, its electronic and microscopic reversibilities under annealing are investigated.

Float-zone 4 $\Omega\cdot\text{cm}$ phosphorus-doped mirror-polished Topsis *c*-Si(100) wafers were used. The surface cleaning consisted of removing the native oxide in a diluted hydrofluoric acid (HF) solution for 45 s. The wafers were then loaded directly into a plasma-enhanced chemical vapor deposition (PECVD) system for intrinsic and doped *a*-Si:H layer depositions. Further details are described elsewhere.^{10,11} For ITO deposition, an MRC 603 magnetron reactive-ion sputtering tool, operated in DC mode, was used with Ar as carrier gas. An additional oxygen flow was introduced to tune the optical and electronic properties of the films. The passivation quality of the *a*-Si:H/*c*-Si interfaces was monitored by measuring τ_{eff} of the samples with the photo-conductance (PC) technique, either in transient or quasi-steady-state mode.¹² In addition, to characterize the microstructure of these thin *a*-Si:H films, attenuated total reflectance (ATR) Fourier transform infrared (FTIR) spectroscopy was used in transmission mode, under nitrogen atmosphere.

We now turn to the origin of the sputter damage, for which symmetric samples of intrinsic *a*-Si:H films (15–20 nm)

TABLE I. Passivation during SHJ cell processing. τ_{eff} was measured at an excess carrier density of 10^{15} cm^{-3} . Note that τ_{eff} of a full device cannot be measured with the photo-conductance decay method because of the metallization present.

	τ_{eff} (ms)	(Impl.) V_{oc} (mV)
After PECVD	5.1	(730)
After sputtering	1.2	(697)
After curing	...	726

^{a)}Electronic mail: benedicte.demaurex@epfl.ch.

on *c*-Si wafers were used, without any doped layers. This structure averts possible thin-film degradation due to Fermi-level-induced lowering of the Si-H bond-rupture energy during annealing,^{13,14} which may otherwise obscure the phenomenon under study. For our passivation samples, ITO sputtering leads to a loss in lifetime of over 90%. We observed no dependency of this damage on the experimentally tested range of sputtering parameters such as the pressure (5–16 mTorr), oxygen partial pressure (0%–3.2%), or power (100–1000 W). However, increasing the *a*-Si:H layer thickness leads to a less severe electronic degradation. Sputtered zinc oxide (ZnO) introduces a similar degradation. By contrast, boron-doped ZnO TCO layers deposited by metal-organic chemical vapor deposition do not lead to passivation losses. Therefore, the observed degradation is likely linked to the sputtering process rather than the specific used TCO material.

Based on the loss in electronic passivation, the sputter damage must be in the form of a deep defect at the interface, most likely the Si dangling bond.^{15,16} The dangling bonds may be created from plasma luminescence (visible or UV) or electron or particle bombardment (neutrals and ions from the gas phase, the sputtering target and their compounds).⁶

In our experiments, the TCO deposition time strongly influences the induced damage, as shown in Fig. 1(a). From this, we conclude that the deposited ITO film starts to shield the surface from the origin of the damage. To test the role of the plasma luminescence, lifetime samples were fabricated which were shielded during TCO sputtering by standard glass (10% transparency at 4.7 eV) or quartz glass (10% transparency at 7.8 eV), or were left bare. Co-deposited lifetime samples showed a reduction in τ_{eff} during sputtering of 14% when shielded by standard glass, 27% when shielded by quartz glass, and 96% when left bare, as shown in Fig. 1(b). During sputtering, the substrate temperature remained below 75 °C in all conditions, excluding thus *in situ* annealing effects. Thus, the damage must be caused at least partially by plasma luminescence, agreeing with Ref. 24. The remaining damage stems from either deeper UV (higher than 7.8 eV) irradiation, or from particle bombardment (energies up to 150 eV).¹⁷ Historically, damage in different types of silicon structures has been reported for both mechanisms: UV light for the creation or activation of deep defects at the silicon dioxide/*c*-Si interface^{18,19} and in amorphous

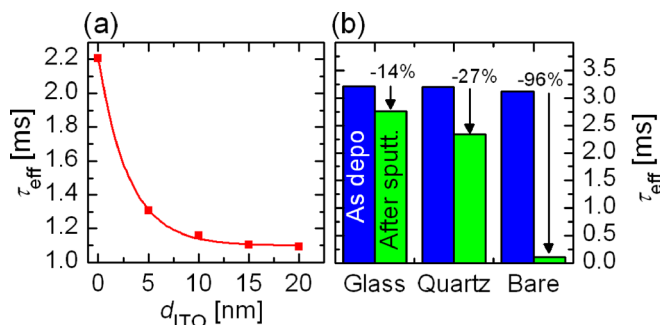


FIG. 1. (a) Effective carrier lifetime of a *n*-type wafer with 20-nm-thick intrinsic *a*-Si:H layers measured as a function of ITO thickness (d_{ITO}), deposited in several steps. (b) Effective carrier lifetime at an excess carrier density of 10^{15} cm^{-3} of a wafer passivated with 15 nm of *a*-Si:H in the as-deposited state and after sputtering protected by glass, quartz, or left bare. The percentages indicate relative losses in lifetime.

hydrogenated silicon nitride;²⁰ and electron²¹ or Ar+ (Refs. 22–24) ion bombardment for the creation of similar defects in *a*-Si:H.²⁵ Further investigations are needed to quantitatively assess the impact of each of these species on the passivation degradation in heterojunction solar cells.

For SHJ devices, since metal paste curing is part of the standard process flow, the reversibility of the sputter-induced defects by annealing is of critical importance. To study the *electronic* reversibility, cycles of sequential ITO deposition, ITO etching, and annealing were performed. The ITO was removed after sputtering but before annealing by using hydrochloric acid (HCl, 16%) or HF (5%) for two reasons. First, the difference in electronegativity between ITO and *a*-Si:H leads to a field effect at the interface, affecting the shape of the lifetime curve. Second, the induced Fermi-level shift at the interface may lower the (deep) defect-formation energy compared to samples without ITO overlayers, obscuring our analysis.^{13,14} With spectroscopic ellipsometry, we verified that no ITO traces remained on the sample and that etching of the *a*-Si:H layer (less than 1 Å removed per HF dip) did not affect the film properties. Moreover, as thin films may degrade under annealing depending on their precise microstructure,¹⁰ a film that withstands prolonged annealing (monotonic improvement in passivation during the cumulated annealing time of the experiment) was selected in order to focus solely on the sputter damage behavior.

Fig. 2 shows three ITO sputtering/ITO etching/annealing cycles. They appear to be electronically reversible, as after a few minutes of annealing (190 °C) the original carrier-lifetime is recovered, even though the lifetime curves for the as-deposited and sputtered/annealed states do not fully superimpose at high injection (data not shown). This suggests changes of properties at the interface. The fact that the final V_{oc} is slightly lower than the *implied*- V_{oc} measured directly after PECVD, as shown in Table I, may rather be explained

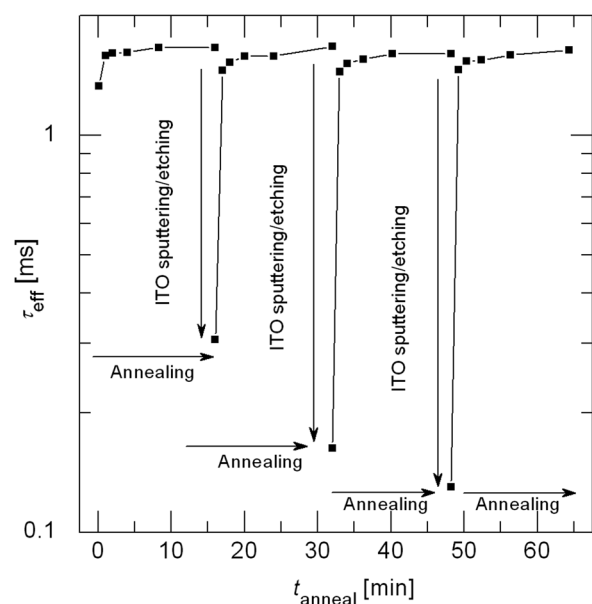


FIG. 2. Effective carrier lifetime of a *n*-type wafer with 20-nm-thick *a*-Si:H layers as a function of cumulated annealing time (t_{anneal}) during repeated ITO deposition/ITO etching/annealing cycles. These cycles show a reversible behavior of the passivation quality.

by the presence of doped layers and TCO in the finished devices, as discussed previously.

The apparent electronic reversibility raises the question whether a corresponding *microstructural* reversibility of the material is present too. Indeed, carrier lifetime measurements probe several nanometers into the *a*-Si:H film bulk starting from the *c*-Si interface.¹⁶ Therefore, most likely, the complete bulk of the films becomes damaged as well, as it sits between the plasma-exposed film surface and the (electronically probed) *a*-Si:H/*c*-Si interface. Linking microstructural and electronic phenomena may elucidate whether dangling bonds originate from the rupture of Si-H or (weak) Si-Si bonds, or both. The energy required to remove a hydrogen atom from an isolated Si-H bond in an *a*-Si:H network is 3.55 eV (Ref. 26) and the energy required to break weak Si-Si bonds is lower (2.5 eV for a strong Si-Si bond²⁷).²⁸ Thus, as many species are present during sputtering with higher energies, both bonds are susceptible to be affected.

To probe the (bulk) Si-H microstructure of the films, ATR-FTIR spectra were recorded on a *c*-Si prism cut from a wafer identical to our carrier lifetime samples and bifacially coated with thin intrinsic *a*-Si:H films. Typically, the hydrogen bonding environment of bulk *a*-Si:H is characterized by high and low stretching modes (HSM at 2070–2100 cm^{-1} and LSM at 1980–2100 cm^{-1}).²⁹ The LSM is a fingerprint for monohydrides, whereas the HSM indicates the presence of (mono- and multi-) hydrides on internal surfaces of nanosized voids in the film.³⁰ Surface hydrides may exhibit additional Si-H stretching modes in the 2080–2135 cm^{-1} range.³¹

Figure 3(a) shows the absorbance signal of an as-deposited sample, deconvoluted into the bulk HSM and LSM responses. Figure 3(b) displays the evolution of the absorbance during a series of sputtering and annealing treatments. Each spectrum represents the change in absorbance relative to the preceding spectrum. Furthermore, before each measurement, the ATR prism was dipped in HF for 30 s to remove ITO (if present) or native oxide, and to ensure consistently identical surface termination. Spectrum (α) shows the absorbance change induced by an HF dip alone. The LSM absorbance is decreased by such etching. Spectrum (β) shows the absorbance difference [relative to spectrum (α)] after sputtering ITO on both faces of a prism protected by quartz. After exposure to the plasma luminescence, the LSM absorbance slightly drops further compared to the effect of an HF etch, whereas the HSM signal hardly changes. Spectrum (γ) shows that bifacial ITO sputtering with no protection induces loss similar to spectrum (β) for the LSM. By contrast, the HSM absorbance drops notably. Apparently electrons, ions, or neutrals in the plasma, or deep UV irradiation decrease the HSM absorbance. Subsequent annealing of the prism (5 min at 190 °C) decreases the LSM absorbance further but increases the HSM absorbance, as shown in spectrum (δ). Conversely, a pristine *a*-Si:H-coated ATR prism exposed to similar annealing does not yield any HSM increase. Thus, the HSM increase after annealing of the sputtered film indicates recovery of the sputter damage. Further annealing of either pristine or sputtered/etched prisms leads to a strong LSM absorbance decrease as well as a HSM absorbance decrease [spectrum (ϵ)]. Figure 3(c) summarizes the passivation quality evolution under the same treatments as in Fig. 3(b).

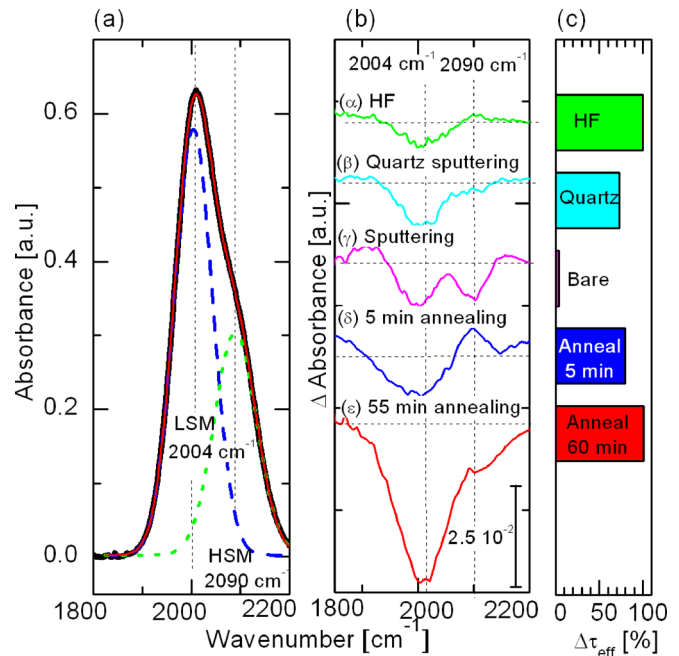


FIG. 3. ATR spectra of 15-nm-thick intrinsic *a*-Si:H films on a *c*-Si wafer. (a) Absorbance spectrum and deconvolution of the LSM and HSM peaks at 2004 cm^{-1} and 2090 cm^{-1} . (b) Difference in absorbance spectra for each step of the experiment. The difference at each step is reported relative to the immediately preceding spectrum. Effect on absorbance of (α) a 30 s HF etch of the *a*-Si:H prism, (β) sputtering both sides of the prism protected by a quartz glass and a 30 s HF etch, (γ) sputtering both sides of the prism with no protection and a 30 s HF etch, (δ) annealing the prism in air for 5 min and a 30 s HF etch, and (ϵ) annealing the prism in air for 55 min and a 30 s HF etch. Curves are offset vertically. (c) Corresponding relative τ_{eff} changes compared to the as-deposited state.

Four key points ensue from our experiments: (1) Sputtering decreases the HSM intensity of an *a*-Si:H film, which may be (partially) recovered by short annealing. (2) Annealing of an as-deposited or sputtered *a*-Si:H film modifies the Si-H bonding configuration of the film (both in HSM and LSM). (3) The film does not regain its initial Si-H bonding state after sputtering and annealing. (4) The microscopic changes in the Si-H stretching modes due to sputtering and annealing do not relate unequivocally to changes in the electronic passivation quality of the interface. Indeed, the changes in the HSM of spectra (γ) and (δ) may be related to the loss and recovery in passivation after sputtering and short annealing. However, under prolonged annealing, the HSM decreases whereas the lifetime increases further. To resolve this apparent paradox, we note that low-energy Ar^+ ions (~ 20 eV) impinging on an *a*-Si:H surface may break Si-H bonds close underneath the surface, rather than deep in its bulk.²² Therefore, the bonding changes seen here after sputtering [spectrum (γ)] may mainly arise from the *a*-Si:H sub-surface region, rather than from the electronically probed *a*-Si:H/*c*-Si interface. However, this does not explain the observed *electronic* changes yet.

Passivation quality may depend on Si-Si bond rupture/formation as much as, or instead of, the Si-H bonding state. Changes in Si-Si bonding are often linked to electronically reversible phenomena in *a*-Si:H. Usually, a weak Si-Si bond ruptures into two dangling bonds, whereupon a nearby bonded H-atom may switch positions with one of the Si dangling bonds for stabilisation. A prime example of this reversible

phenomenon is the light-induced Staebler-Wronski effect (SWE),³² also observed recently at *a*-Si:H/*c*-Si interfaces.^{33,34} Si-Si bonding is not observable with FTIR due to bond symmetry. The data in Fig. 3(b) show that, upon annealing, permanent changes in the Si-H vibration intensity occur. Importantly, such changes could be not only due to Si-H bond rupture but also to changes in dielectric environment (such as due to bond switching) without actual deep-defect generation.^{27,35} However, the discrepancy between electronic reversibility and microstructural irreversibility during annealing suggests that Si-Si bond formation dictates the electronic trends at the interface in these films, rather than Si-H reformation.

To summarize, sputtering degrades the electronic passivation quality of the *a*-Si:H/*c*-Si interface. Dangling bonds are created at least partially by plasma luminescence. From an electronic point of view, these defects appear to be mostly reversible under low-temperature annealing. Despite this, permanent microscopic changes in the *a*-Si:H network, involving Si-H bonds, are observed after sputtering and subsequent annealing. The as-deposited film's microstructure cannot be fully recovered. Nevertheless, with device-grade films, we do not observe a notable loss in device V_{oc} , suggesting that the passivation quality may not be directly dictated by the film microstructure.

The authors gratefully acknowledge Loris Barraud, Jonas Geissbühler, and Johannes Seif for their technical contribution and fruitful discussions, as well as Jakub Holovsky for the ATR-FTIR setup. This work was partially supported by Axpo Naturstrom Fonds by the European Commission's 7th FP [FP/2007-2013] under the 20 Plus Project (Grant Agreement No. 256695) and by the Swiss Federal Office for Energy.

¹T. Mishima, M. Taguchi, H. Sakata, and E. Maruyama, *Sol. Energy Mater. Sol. Cells* **95**, 18 (2011).

²S. De Wolf, A. Descoedres, Z. H. Holman, and C. Ballif, *Green* **2**, 7 (2012).

³M. Tanaka, M. Taguchi, T. Matsuyama, T. Sawada, S. Tsuda, S. Nakano, H. Hanafusa, and Y. Kuwano, *Jpn. J. Appl. Phys.* **31**, 3518 (1992).

⁴A. Descoedres, Z. C. Holman, L. Barraud, S. Morel, S. De Wolf, and C. Ballif, ">21% efficient silicon heterojunction solar cells on n- and p-type wafers compared," *IEEE J. Photovoltaics* (in press).

⁵T. F. Schulze, H. N. Beushausen, C. Leendertz, A. Dobrich, B. Rech, and L. Korte, *Appl. Phys. Lett.* **96**, 252102 (2010).

⁶A. Plagemann, K. Ellmer, and K. Wiesemann, *J. Vac. Sci. Technol. A* **25**, 1341 (2007).

⁷R. Street, D. Biegelsen, and J. Stuke, *Philos. Mag. B* **40**, 451 (1979).

⁸M. Lu, S. Bowden, U. Das, and R. Birkmire, *Appl. Phys. Lett.* **91**, 063507 (2007).

⁹D. Zhang, A. Tavakoliyaraki, Y. Wu, R. A. C. M. M. van Swaaij, and M. Zeman, *Energy Proc.* **8**, 207 (2011).

¹⁰A. Descoedres, L. Barraud, R. Bartlome, P. Bôle, G. Choong, S. De Wolf, F. Zicarelli, and C. Ballif, *Appl. Phys. Lett.* **97**, 183505 (2010).

¹¹A. Descoedres, L. Barraud, S. De Wolf, B. Strahm, D. Lachenal, C. Guerin, Z. C. Holman, F. Zicarelli, B. Demaurex, J. Seif, J. Holovsky, and C. Ballif, *Appl. Phys. Lett.* **99**, 123506 (2011).

¹²R. A. Sinton and A. Cuevas, *Appl. Phys. Lett.* **69**, 2510 (1996).

¹³S. De Wolf and M. Kondo, *J. Appl. Phys.* **105**, 103707 (2009).

¹⁴T. Koida, H. Fujiwara, and M. Kondo, *Appl. Phys. Express* **1**, 04501 (2008).

¹⁵S. De Wolf, S. Olibet, and C. Ballif, *Appl. Phys. Lett.* **93**, 032101 (2008).

¹⁶S. De Wolf, C. Ballif, and M. Kondo, *Phys. Rev. B* **85**, 113302 (2012).

¹⁷Y. Tagaki, Y. Sakashita, H. Toyoda, and H. Sugai, *Vacuum* **80**, 581 (2006).

¹⁸D. Reinwand, M. Graf, P. Hartmann, R. Preu, and R. Trassl, in *Proceedings of the 25th European Photovoltaic Solar Energy Conference and Exhibition* (WIP, Munich, Germany, 2010), p. 1908.

¹⁹P. E. Gruenbaum, R. R. King, and R. M. Swanson, *J. Appl. Phys.* **66**, 6110 (1989).

²⁰J. Kanicki, W. L. Warren, C. H. Seager, M. S. Crowder, and P. M. Lenahan, *J. Non-Cryst. Solids* **137–138**, 291 (1991).

²¹H. Schade and J. I. Pankove, *J. Phys. Colloques* **42**, C4-327 (1981).

²²W. M. M. Kessels, D. C. Marra, M. C. M. van de Sanden, and E. S. Aydil, *J. Vac. Sci. Technol. A* **20**, 781 (2002).

²³R. Durny, E. Pincik, V. Nadazdy, M. Jergel, J. Shimizu, M. Kumeda, and T. Shimizu, *Appl. Phys. Lett.* **77**, 1783 (2000).

²⁴A. Illiberi, P. Kudlacek, A. H. M. Smets, M. Creatore, and M. C. M. van de Sanden, *Appl. Phys. Lett.* **98**, 242115 (2011).

²⁵In our experiments, we observed a drop in lifetime of 92% for an unprotected sample, and of 15% with glass protection, when exposed to an Ar plasma in a PECVD system.

²⁶C. Van de Walle and R. A. Street, *Phys. Rev. B* **51**, 10615 (1995).

²⁷R. B. Wehrspohn, S. C. Deane, I. D. French, I. Gale, J. Hewett, M. J. Powell, and J. Robertson, *J. Appl. Phys.* **87**, 144 (2000).

²⁸M. Stutzmann, W. B. Jackson, and C. C. Tsai, *Phys. Rev. B* **34**, 63 (1986).

²⁹A. A. Langford, M. L. Fleet, B. P. Nelson, W. A. Lanford, and N. Maley, *Phys. Rev. B* **45**, 13367 (1992).

³⁰A. H. M. Smets, W. M. M. Kessels, and M. C. M. van de Sanden, *Appl. Phys. Lett.* **82**, 1547 (2003).

³¹M. Z. Burrows, U. K. Das, R. L. Opila, S. De Wolf, and R. W. Birkmire, *J. Vac. Sci. Technol. A* **26**, 683 (2008).

³²D. L. Staebler and C. R. Wronski, *Appl. Phys. Lett.* **31**, 292 (1977).

³³S. De Wolf, B. Demaurex, A. Descoedres, and C. Ballif, *Phys. Rev. B* **83**, 233301 (2011).

³⁴B. Hekmatshoar, D. Shahrjerdi, M. Hopstaken, and D. Sadana, in *IEEE International Reliability Physics (IRPS)*, IRPS11-562, 2011.

³⁵S. Oguz, D. A. Anderson, W. Paul, and H. J. Stein, *Phys. Rev. B* **22**, 880 (1980).